

# OPEN LoRaWAN SENSOR NODE ARCHITECTURE FOR AGRICULTURE APPLICATIONS

Philipp Bolte<sup>1</sup>, Ulf Witkowski<sup>1</sup> and Rolf Morgenstern<sup>2</sup>

<sup>1</sup>Department of Electronics and Circuit Technology,  
South Westphalia University of Applied Sciences, Soest, Germany

<sup>2</sup>Department of Agriculture, South Westphalia University  
of Applied Sciences, Soest, Germany

## **ABSTRACT**

*In agriculture, it becomes more and more important to have detailed data, e.g. about weather and soil quality, not only in large scale classic crop farming applications but also for urban agriculture. This paper proposes a modular wireless sensor node that can be used in a centralized data acquisition scenario. A centralized approach, in this case multiple sensor nodes and a single gateway or a set of gateways, can be easily installed even without local infrastructure as mains supply. The sensor node integrates a LoRaWAN radio module that allows long-range wireless data transmission and low-power battery operation for several months at reasonable module costs. The developed wireless sensor node is an open system with focus on easy adaption to new sensors and applications. The proposed system is evaluated in terms of transmission range, battery runtime and sensor data accuracy.*

## **KEYWORDS**

*Wireless Sensor Node, LoRa Communication, Real-Time Environmental Monitoring, Urban Agriculture.*

## **1. INTRODUCTION**

The success of crop farming is traditionally dependent on weather and climate patterns. Farmers have a long history of weather and climate observation as well as weather prediction, formerly based on local experience and intuition, later augmented with systematic weather data collection and forecasting by agricultural and national institutions. Research on low precipitation and drought of the recent years has revealed a strong spatial diversity [1]. This can mean that some plots of land received sufficient rainfall, but adjacent plots suffered from water shortage. Micro climates in cities can lead to similar effects. This situation generates the desire of field scale data acquisition for farmers to allow for adapted irrigation measures.

The coarse scale of data acquisition is being augmented with fine grained and more detailed data, not only concerning weather and climate parameters, but also soil and plant data, in the precision farming movement. This is even more important for Urban Agriculture (UA) where the plots are very small and scattered in the urban landscape. Partial shading and the structure of surrounding buildings create microclimates that may differ widely between plots even though they are not very far apart.

The generally small total size of an UA operation requires an urban farmer to minimize waste and transportation and to maximize yield as well as farmer and staff productivity. Hyper local environmental, soil and plant data, possibly extended with presence and intrusion detection can facilitate the complex crop and harvest planning and general farm management task. Ideally plots are monitored on an individual basis.

### **1.1. Application Scope**

Urban Farming oftentimes employs different production techniques, adapted to local conditions of the production locations. Market gardening, also known as Small Plot INTensive (SPIN) farming on open plots, is often enhanced with simple foil tunnels or small scale greenhouses. Increasingly Hydroponics and Aquaponics are utilized in order to produce in locations that do not offer arable soil [2]. These water based production methods require the monitoring of relevant water parameters like temperature, electronic conductivity (EC) and pH of the nutrient solution as well as the dissolved oxygen (DO) when fishes are involved. The welfare of the fishes in the aquaculture of such a system calls for near real-time monitoring of the mentioned parameters.

The collection of different environmental and production system parameters, that are relevant for such an operation, range from air temperatures and relative humidity over soil temperature and moisture, global radiation and daily light integral (DLI) to the mentioned process water parameters. The design of a hydroponic or aquaponic system might additionally require liquid flow and liquid level measurements. Finally, location detection of equipment and presence detection of staff as well as intrusion detection add one more dimension to be monitored.

Production plots are usually not all located in the direct vicinity of a building the farmer has authority over. On a case to case basis it might be possible to ask friendly neighbours for Wi-Fi connectivity to have wireless access to sensor devices. But this approach bears the risk of depending on a crucial part of the management infrastructure not being under control of the farmer. Therefore, alternative methods for data transportation from the field or greenhouse to the data management application are desirable.

### **1.2. Typical Requirements**

The usage of data logging systems for agriculture application is associated with application specific requirements. The typical users of such systems do not have extensive technical expertise. Therefore, the deployment and particularly the maintenance of data logging systems and related sensors must be simple. A large battery lifetime is expected. The sensors are often placed in harsh conditions exposed to rain, condensing humidity and sun light exposure.

It must be distinguished between short term usage and continuous monitoring applications. In research the experiments are usually time limited and technical experienced staff is available. The overall requirements of the sensor system are not nearly as extensive compared to long-term usage. The availability of real-time data over long time periods promise benefits in the areas of food safety, cost reduction, operational efficiency and asset management [3]. Current research is furthermore utilizing machine learning to control the process aiming additional yield optimization using real-time data [4].

#### **1.2.1. Sampling Frequency**

Growing crops and fattening fish are rather slow processes that do not generally require real-time data acquisition or high sampling frequencies. Depending on the local context, sampling times between one minute and one hour should be sufficient for the bulk of applications. Suitable

transmission frequencies might even be lower than one per minute or one per hour if data is buffered in the sensor node. Two applications however benefit from near real-time sampling and transmission: vital water parameters for the aquaculture and intrusion detection. Low oxygen supply in the aquaculture requires an immediate action of the farmer as ensuring the welfare of animals in husbandry is not only necessary to mitigate the risk of losses, but also a legal requirement. The rationale for a timely reaction to an intruder is self-explanatory.

### **1.2.2. Transmission Distances**

Sensor data needs to be transmitted over distances well beyond the range of conventional Wi-Fi networks. In agricultural settings fields are usually in a distance between 2 and 7.5 kilometres from the farm [5]. In urban agriculture scenarios production plots are typically between one to three kilometres apart [6]. Urban environments present an additional level of difficulty with buildings obstructing the line of sight between transmitter and receiver of a setup, lowering the signal quality and the maximum range of the chosen transmission technology [7].

### **1.2.3. Environmental Conditions**

Sensors nodes and transmission equipment are exposed to outdoor conditions, with seasonally varying temperature ranges, rain and wind. Sensors placed in protected production facilities like greenhouses and foil tunnels can be exposed to elevated temperatures as well as to condensing humidity. Greenhouses and foil tunnels might additionally complicate the RF situation when the metal structure acts like a Faraday cage, dampening signal strength and distorting the signal.

### **1.2.4. Usability**

Farmers and urban farmers are typically no experts in information technology. While both profession groups usually need to be able to adapt technology to their production intents, it is desirable for a sensor network setup to be as easy to deploy and to maintain as possible. The battery runtime of the sensor must exceed several months. Integrating additional sensors into a system should pose a low barrier. Urban Farming environments might require temporarily shifting sensors to new plots, helping the farmer to grasp the local conditions, allowing him to adapt the production concept accordingly.

## **1.3. Structure of the Paper**

In Chapter 2 the current state of the art of data logging systems is presented. The features of the currently used technologies for data transmission of sensor nodes (SN) are compared. The potential for novel LoRaWAN based SN is highlighted. The overall system architecture is explained in Chapter 3. The focus of this chapter is on the data routing between the SN and the cloud application. The structure of proposed sensor node is explained in detail in Chapter 4. The used hardware and software components are introduced. A simplified device configuration approach and measurements for power consumption reduction are explained.

This work evaluates if the proposed sensor node is suitable for the use in UA applications in terms of provided range, battery runtime, and sensor accuracy. The range evaluation is performed in Chapter 5. Signal strength and quality parameters were recorded and evaluated for different locations. In Chapter 6 the battery runtime was analysed. A power interval analysis shows the current consumption for the different operating modes of the SN. The theoretical battery lifetime was estimated using the results from the power interval analysis. This estimation was validated and confirmed by an experiment. An accuracy evaluation of supported temperature and humidity sensors is performed in Chapter 7. Those physical quantities are essential in many UA

applications and are well assessable. The measured sensor values are compared to data from a professional weather station to gather the statistical parameters of the used sensors. A conclusion and suggestions for further research are given in Chapter 8.

## 2. STATE OF THE ART

A variety of different data logging systems are used in the agricultural sector. Different categories of devices are discussed in this section. Their usage depends mainly on the need for real-time data access, the requirements on simplicity and the duration of usage.

### 2.1. Offline Data Logging

Offline data loggers store measurement data locally. The data inventory needs to be read out manually. Those data loggers are available from 50\$ to 2000\$ with respect to functionality, the size of data storage and battery lifetime. The configuration and installation of these devices is usually simple compared to setup of wireless sensor networks (WSN). No communication network infrastructure or mains supply is required for operation. This type of data acquisition is typically used as a robust and yet simple solution if no real-time data is required. The missing capability of live data transmission and analysis therefore restricts the use cases substantially. Those systems achieve a typical battery lifetime of more than one year as a result of the lacking power intensive radio frequency (RF) transmissions [8, 9].

In other literature those devices are frequently used for time limited experiments, particularly due to the extensive effort of the manual data readout. Shaw et. al. are using an offline DL2e DeltaT data logger to estimate the spatial nitrogen variation within a grassland field [10]. Chatterjee, Dey and Sen developed a neural network based soil moisture quantity prediction model gathered from data using an offline HOBO U30 data logger [11].

### 2.2. Cellular Connected WSN

Data loggers with a cellular modem solve the problem of lacking online data. Those devices transmit the measurements periodically using a mobile radio. Common variants are using GSM, 2G or 3G cellular network technology which are not low-power optimized. Those systems have a fairly high power consumption when transmitting [12] and often require a mains power supply [13]. Currently new cellular technologies optimized for IoT applications are emerging. The LTE-Cat-NB1 and LTE-Cat-M1 extensions provide a narrow-band data transmission optimized for low-power and high range utilizing existing infrastructure [14]. Zhang et. al. proposed a sensor node equipped with an LTE NB-IoT modem for data transmission that transmits environmental parameters at an interval of one week with an estimated battery lifetime of 11 years [15]. Those systems still need a registered SIM card introducing recurring costs. As with all cellular networks the usage is limited to areas with actual network coverage. A basic LTE NB-IoT network coverage of Telekom in Germany at January of 2021 is given but especially rural parts are still lacking connectivity [16].

The proprietary SigFox network pursues a similar approach as the IoT optimized LTE protocols. A narrow-band technology is utilized for low bandwidth data transmission over long distances. The creator of the SigFox protocol acts as the only available provider of this technology at the same time. The costs of the service depend on the number of devices and the frequency of message transmission. The network coverage in Germany is especially problematic in rural areas [17]. The Thoreau project uses the SigFox network to transmit underground soil moisture and ambient temperature data from sensor nodes installed on multiple location on a campus into a

cloud application over long time periods [18]. Joris et. al. are using a solar powered SigFox sensor node to transmit temperature and humidity measurements on a vineyard to evaluate the weather influence on the yield [19]. The usage of cellular data loggers is introducing a dependency to 3rd party network providers. This should be specially considered for long term usage scenarios. The provider may increase the usage fees or even shut down the service in non-profitable situations.

### **2.3. UAV Supported Data Logging**

A new approach is using autonomous drones for the readout of data loggers. A drone is used to temporarily activate a communication interface of the data logger using RF pulses [20]. The short distance between the data logger and the drone enables the usage of ultra-low power RF protocols for measurement data transmission providing only a short range [21]. Those systems could be extended by path planning techniques to automate the control of the drone that were designed for similar problems [22, 23]. Idbella et al. presented such a UAV based data logging approach for monitoring agro-ecological condition of vine plants [24]. In this experiment the placement of sensors and the control of the drone was performed manually. More research is necessary to adapt existing path planning techniques to this specific problem. This ambitious approach for sensor data collection is still in development. Particular aspects are already working but the challenge here is the integrating of sensor technology and complex automated control of the UAV into a usable product at reasonable costs. Real time data acquisition would still not be possible with this approach and the costs for the required infrastructure is fairly high compared to traditional WSN.

### **2.4. LoRaWAN connected data logging**

A promising technique for low-power and long-range data transmission in agricultural applications is LoRaWAN. Data loggers equipped with a LoRaWAN modem were already used for experiments and show good results. Davcev et al. are utilizing a LoRaWAN technology from The Things Network to measure leaf wetness and soil moisture to control an irrigation system [25]. The focus of that research however was on the data analytic part of the system. Ibrahim et al. are using LoRaWAN development kits to measure and control the ambient humidity of a Shiitake fungi cultivation [26].

Those experiments are using LoRaWAN implementations that are not optimized for general agriculture applications. The used hardware was tailored to the specific experiments and does not provide a generalized interface for sensors. Furthermore, aspects as power consumption and range were not a focus of that work. The LoRaWAN technology itself is a promising approach if real-time data is required. The low-power narrow-band RF transmission enable small sensor nodes with a large battery lifetime while using a high sampling rate. The capability of self-deployment of gateways enable good network coverage even in rural areas and decouples the dependence of 3rd party providers.

## **3. SYSTEM ARCHITECTURE**

The proposed sensing and data logging system is a wireless sensor network (WSN) using LoRaWAN technology as RF protocol to connect the sensors to a gateway, as shown in Figure 1. The architecture is made of three layers. The sensor data is gathered by the SN in the bottom layer. The network layer is using LoRaWAN technology for routing and aggregation of the sensor data into the application layer. Here, the gateway (GW) aggregates the data from the

sensor nodes. The data storage, analysis and representation is realized as a cloud service in the application layer. Those layers are described in more detail in the following subsections.

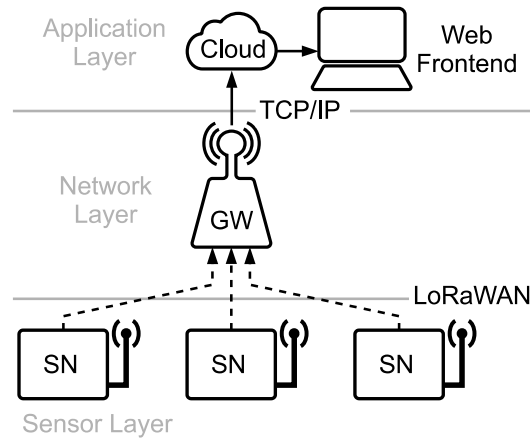


Figure 1. Overall system overview of the wireless sensor network with cloud integration

### 3.1. Data Routing and Aggregation

The measurement data is transmitted from the sensor to the application layer using LoRaWAN technology utilizing LoRa RF modulation. The physical layer of data transmission is using the proprietary narrow-band LoRa protocol from Semtech. The direct sequence spread spectrum (DSSS) is replacing each bit by a sequence of bits resulting in a signal with higher bandwidth that is less prone to narrow-band interference. Chirp spread spectrum (CSS) transmits each symbol using continuously varying frequency to eliminate the need for a precise reference clock [27]. The modulation provides a high range while using less energy though only achieving relatively low data rates. The specified LoRa modulation describes the raw RF transmission only. The adaption of parameters (e.g. spreading factor, bandwidth) enables a trade-off between range and data rate. More advanced features are implemented in the upper LoRaWAN layer.

The medium access control (MAC) and the aggregation and routing of messages is done using the LoRaWAN protocol extension. The data transfer is always initiated by the end devices (SN) followed by a receiving window for data uplink from the network [28]. The end devices stop listening after the receiving windows and enter a sleep state to save energy. Messages from a single or multiple gateways are aggregated by a central network server (NS) and from there redirected to specific application servers (AS) both using TCP/IP based protocols, as shown in Figure 2. The LoRaWAN infrastructure can be self-supplied by the operator of the network or a third party provider can be used. We are using the infrastructure from The Things Network (TTN) for the proposed WSN. TTN offers a free usage of their infrastructure. Therefore, the gateways need to be connected to their service. The gateway is then available for all registered TTN users. The motivation of TTN is to create a global LoRaWAN network only with community operated gateways. The separate encryption of payload and network metadata should prevent eavesdropping.

### 3.2. Application Layer

In the application layer all received sensor data is processed and stored depending on the specific application. In our setup the aggregated messages are fetched by a Node-RED instance from TTN by using the MQTT protocol, shown in Figure 2. Node-RED is a web-based tool for data

processing. The graphical flow-based approach allows a simple design of rules for data processing [29]. For the proposed architecture the received measurement data is validated and stored in an InfluxDB database. The Node-RED software provides interfaces for MQTT and InfluxDB.

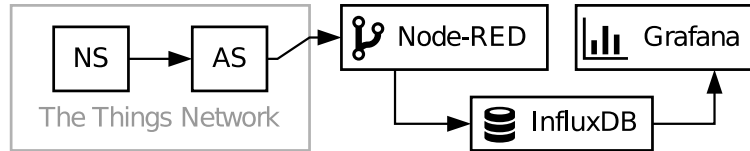


Figure 2. Application structure for data aggregated by a LoRaWAN network

The used InfluxDB time series database (TSDB) is specialized for storing periodical data. Compared to traditional relational database management systems (RDBMS, e.g. MySQL) the performance for storing single measurements is significant higher [30].

One crucial aspect of the overall system is the easy evaluation and processing of the measurements. The web-based Grafana frontend allows a simple query of the recorded measurements [31]. A visualisation using graphs (e.g. lines, bars, points), gauges, tables and integration of third party controls is supported. The user can set the time range of the output data. It is possible to show simple statistical data (min, max, average, sum) in a legend. Thresholds can be set to visualize critical periods and to send alerts via E-Mail. The graph raw-data can be exported to CSV files for further processing.

#### 4. SENSOR NODE ARCHITECTURE

The major effort of the proposed system was put into the adaption of the developed IoTye sensor node (SN) supporting LoRaWAN for agriculture applications. This SN architecture was originally developed by our faculty as a generic LoRaWAN sensor platform. This work optimizes the software stack in terms of easy deployment and simplified sensor inclusion. Figure 3 shows the logical structure of the proposed SN. Main processing component is the STM43L4 MCU. It supports multiple low-power states while providing high processing power if required. A trade-off between low power-consumption and computing power in active state is achieved by a flexible clock selection. The used sleep mode (Stop 2) consumes  $2.4\mu\text{A}$  with enabled real-time clock (RTC) and backup memory.

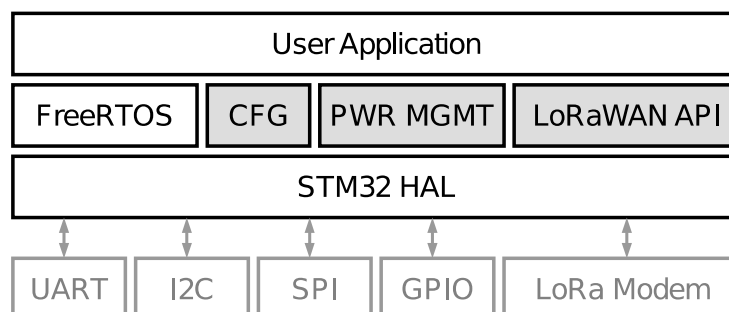


Figure 3. Sensor node stack of the IoTye device

The sensors are physically connected to the various interfaces of the MCU. The STM32 HAL library from STMicroelectronics provides high-level hardware drivers for the MCU core and the peripherals. FreeRTOS is used as a real-time operating system for scheduling multiple tasks and synchronizing shared resources. The grey shaded boxes, these are CFG (configuration parser), PWR MGMT (power management unit), LoRaWAN API (LoRaWAN driver) are self-developed parts of the SN framework. These components are introduced in the following sections. Different parts of the developed software are implemented in dedicated tasks to improve the modularity of the software project and to ease code maintenance.

#### 4.1. Program States

The software supports periodic data readings from the sensor devices via different interfaces, node integration into the sensor network, data transmission, and low-power sleep modes. The program flow of the SN is predefined by the developed software framework according to Figure 4.

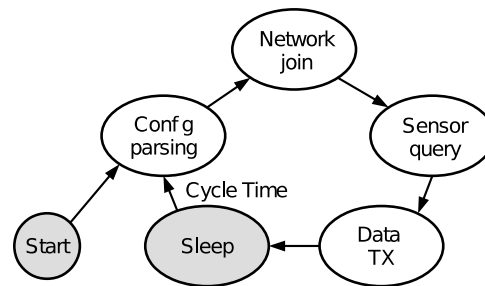


Figure 4. Program states of the sensor node

The system first parses the configuration file stored on the EEPROM. This step includes the recovery of persistent application data from the backup RTC RAM. This data is empty at first start. Afterwards the SN joins the LoRaWAN network, see 4.3 for detailed description. All enabled sensors are initialized and read out. The collected measurements are transmitted using the LoRaWAN modem. Finally, the device is set into a low-power sleep state to reduce the power consumption. The SN restarts after a configurable cycle time. The sleep state is also set on network errors. Unsuccessful measurements do not interrupt the program and only set a failure flag in the payload data to mark the certain measurement as invalid.

#### 4.2. Configuration Management

The implemented configuration management provides a simple mechanism for storing application specific parameters. The configuration includes all connected sensors and their parameters (e.g. interface, slave address), the measurement interval and LoRaWAN related specifications (e.g. device EUI, application EUI, encryption keys, data rate). The configuration needs to be set during the deployment of the SN. Figure 5 shows the structure of the implemented configuration management.

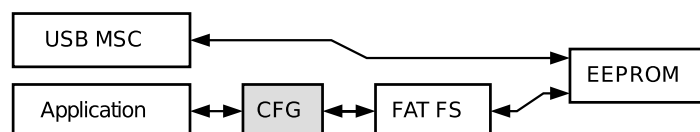


Figure 5. Configuration management of the sensor node



The configuration is stored in a text file on a FAT32 formatted I<sup>2</sup>C EEPROM. The file access on the MCU is provided by the used FAT FS library. The implemented configuration parser (CFG) retrieves the individual parameters to the application. The configuration file can be changed by connecting the SN to a computer using the provided USB interface. The SN implements the USB mass storage device class (MSC) that maps the EEPROM as a drive on the computer. Therefore, it is possible to change the configuration file with a regular text editor. Furthermore, a prepared file can be easily copied to the drive simplifying mass deployment. The utilization of the USB MSC standard provides OS independent compatibility and eliminates the need for a dedicated configuration software and hardware programmer.

### 4.3. LoRaWAN Driver

One module of the software stack is the LoRaWAN driver, cf. LoRaWAN API in Figure 3. This driver provides an API to the application that enables a simplified connection management and data transmission. The low-level driver manages the UART interface between the MCU and the LoRaWAN modem. The high-level driver transmits AT commands, parses the response and implements the state management. An API is declared to the application for simple usage of the LoRaWAN network.

LoRaWAN clients usually perform an over the air activation (OTAA) to join the network after each power-up. The clients send a join request and the gateway answers with a join accept response including a nonce for generation of the session keys for data encryption. The generated session keys are usually lost after power-down. The developed driver stores the session keys in the modem for reuse. The OTAA is replaced by activation by personalization (ABP) if session keys are present. The ABP approach does not require any join request, thus reducing the required duty cycle of the SN for subsequent measurements. An OTAA is only performed at the first start or if the ABP method fails (e.g. if the NS rejected the session keys after long inactivity). A cyclic regeneration of the session keys by performing OTAA can be optionally scheduled by the application developer to improve the security if required.

### 4.4. Power Management

A long battery lifetime is achieved by entering a low-power mode between the measurements. The software stack includes a dedicated power management (PWR MGMT) module to simplify the usage of low-power states for the application developer. All required setups are executed before entering the low-power state. This covers platform (e.g. power-down of LoRaWAN modem) and MCU (e.g. interrupt configuration) specific tasks and the configuration of the wake-up source. The Stop 2 state of the MCU with enabled RTC is entered between the measurements. The RAM is disabled when entering this state to reduce the power consumption to a minimum. The MCU is therefore rebooting after wake-up. The PWR MGMT module provides a mechanism to store application specific data into the backup memory of the RTC. The data is passed as a structure to the PWR MGMT module before entering the low-power state and is retrieved after the MCU is rebooted. This allows the application developer to store data between the measurement cycles.

### 4.5. Sensor Drivers

The modular system architecture allows a simple integration of sensor drivers using the C programming language. The included STM32 HAL library offers high-level access to all peripherals of the MCU. Platform specific example code for various interfaces (GPIO, ADC, I<sup>2</sup>C, SPI, UART) is available. The SN software framework includes drivers for various sensors that can be used in the application layer. Table 1 shows all provided sensor drivers.

Table 1. By SN supported sensor devices with related interfaces

Sensor	Physical quantities	Interface
DHT22 / AM2303	Temperature + r.H.	GPIO
Sensirion SHT21	Temperature + r.H.	I <sup>2</sup> C
Sensirion SHT31	Temperature + r.H.	I <sup>2</sup> C
Texas Instruments HDC1008	Temperature + r.H.	I <sup>2</sup> C
Maxim DS18B20	Temperature	GPIO
Bosch BMP280	Pressure + temperature	I <sup>2</sup> C
Bosch BME680	Press. + temp. + VOC	I <sup>2</sup> C
TAOS TSL2561	Luminosity	I <sup>2</sup> C
Capacitive Soil Moisture	Soil moisture	Analog
Sparkfun Soil Moisture	Soil moisture	Analog
Nova SDS010	Particulate matter	UART
Sensirion SPS30	Particulate matter	UART
Sensirion SCD30	CO2 + temp. + r.H.	I <sup>2</sup> C

A template for developing a custom driver is additionally provided. A separation between the low-level hardware access and the device logic is introduced. Each part is implemented in a separate pair of .c/.h files. The programmer can utilize the synchronization functions and blocking delays from FreeRTOS eliminating the need of implementing own schedulers. The high-level functions are called from the application layer.

#### 4.6. Reference Hardware

The described architecture is implemented in a reference hardware. Core component of the SN is the IoTyze LoRa board extended by various peripherals as shown in Figure 6.



Figure 6. Reference hardware of the sensor node

This credit card sized board integrates an STM32 host MCU, an RN2483 LoRaWAN modem and a power management system with lithium polymer (LiPo) battery charger [32]. The SN is supplied by one 3.7V LiPo cell with 2200mAh capacity. The system is mounted inside an IP65 classified case to provide a protection against external environmental influences. The USB interface used for device configuration and battery charging is realized using a robust aviation-grade GX12 connector. The sensors are connected using similar GX12 connectors. Those

measures prevent the entry of moisture. The SN can be mounted in environments facing splashing water (e.g. outdoor) or condensing humidity (e.g. green houses).

## 5. RANGE EVALUATION

The achieved range depends on the transmission power of the transmitter and used data rate. The data rate of a LoRa system depends on the used bandwidth and spreading factor (SF). The SF determines the required SNR at the receiver until demodulation becomes possible. The receiver sensitivity is given by Equation 1 [33].

$$S = -174\text{dB} + 10 \log BW + NF + SNR \quad (1)$$

where,

- $S$  = Receiver sensitivity
- $BW$  = Bandwidth
- $NF$  = Noise figure
- $SNR$  = Required signal-to-noise ratio

The bandwidth of LoRa modulation for Europe is fixed to 125kHz, while other parts of the world may use 250kHz [34]. The NF describes the inherent noise of the receiver. The only controllable factor is the used SF resulting in the minimum required SNR. The choice of SF influences the data rate. The use of high SF allows large coverage but reduces the possible data throughput. Table 2 shows minimum required SNR and achievable data rates (DR) for various SF.

Table 2. Resulting SNR and data rates for various SF using LoRa

SF	7	8	9	10	11	12
SNR (dB) [36]	-6	-9	-12	-15	-17.5	-20
DR (kb/s) [27]	5.47	3.13	1.76	0.976	0.537	0.293

### 5.1. Experimental Setup

For range evaluation the sensors were placed at different spatial conditions. Multiple LORIX One gateways are placed at a different position on the campus [35]. The measurements are only recorded from a single GW that was placed at a fixed position. A test software was developed to gather signal strength and transmission quality data. The received signal strength indicator (RSSI) and SNR from the GW is fetched for 100 sequent uplink packages. Each uplink package from the SN is confirmed by a downlink package from the GW. The test was done in a multi gateway environment. The downlink messages are sent by the GW with the best link to the SN. The SNR measurements by the SN were dropped in this evaluation, because the downlink messages are not sent by the same GW for each uplink package that affects the transmission quality. In total, four different spatial setups have been used:

#### Location 1 (indoor, 40m, NLOS):

The test SN was placed indoor in a distance of 40m to the GW. Several thick stone walls are located between the SN and the GW causing additional damping. The signal is partly reflected at the walls, introducing reflection of the transmitted signals.

**Location 2 (outdoor, 200m, LOS):**

The SN was placed outside on the campus in line of sight (LOS) condition to the GW. The distance between the SN and the GW was 200m. The SN was orientated almost straight to the window.

**Location 3 (outdoor, 200m, NLOS):**

In this scenario the SN was placed outdoor in a distance of 200m on the campus with one building between the GW. The signal has to pass multiple walls. Furthermore, the SN was placed angular to the window where the GW was located, requiring the signal to pass part of the facade.

**Location 4 (outdoor, 300m, NLOS):**

The SN was placed at the location on the campus with the distance of 300m to the GW. Three buildings are located between the SN and the GW.

**5.2. Results**

Figure 7 shows the results for location 1. The measured RSSI for all chosen SF are in the range between -84,79dB and -81,45dB. The RSSI measurements show a wider spread for SF of 10 and SF of 11. The average SNR values are in a range from 7,33dB for SF of 12 to 10,28dB for SF of 8.

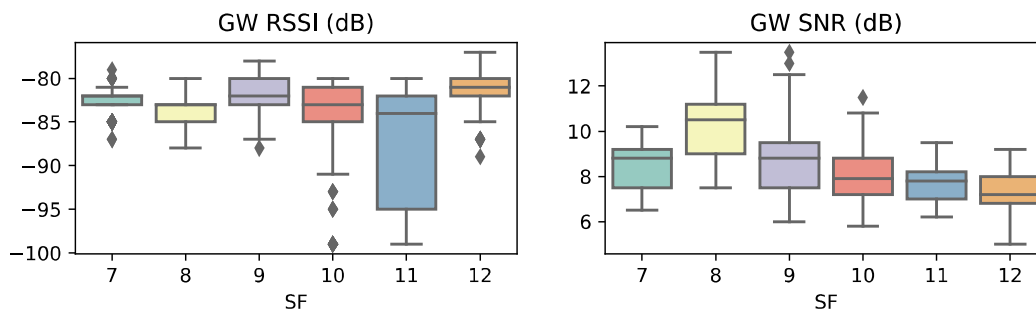


Figure 7. RSSI and SNR measurements at gateway for location 1

The results for location 2 are shown in Figure 8. The range of average RSSI values was between -109,65dB for SF of 11 and -107,92dB for SF of 12. The distribution of single measurements is, again, wider for SF of 10 and SF of 11. The lowest SNR average of 2,17dB was measured for SF of 12 and the highest SNR average of 4,05dB was reached for SF of 10. The SNR values are wider distributed for this location. As expected, the RSSI as well as the SNR are smaller compared to setup in location 1, because of the larger distance between SN and GW.

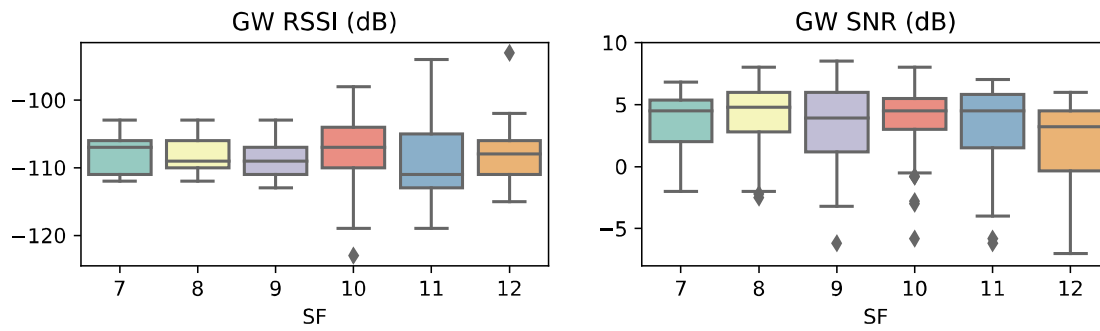


Figure 8. RSSI and SNR measurements at gateway for location 2

Figure 9 shows the result for location 3. The locations 2 and 3 are both located in a distance of 200m to the GW. While location 2 was in LOS to the GW, multiple walls causing a NLOS condition for location 3. For SF of 12 a loss of 7 packets was detected. The RSSI average values are closely around -112dB for all SF. The RSSI measurements are showing more outlier, compared to location 2. The lowest SNR average of -4,09dB was determined for SF12 and the highest average SNR was -2,28dB for SF9. The SNR values are wider distributed for location 3.

The average RSSI and SNR values have slightly deteriorated for NLOS conditions. The distribution of the single measurements is noticeably wider for NLOS conditions, compared to the values for LOS conditions of the same distance. Reflecting signals from the walls, resulting in a multipath effect, could be an explanation for this observation.

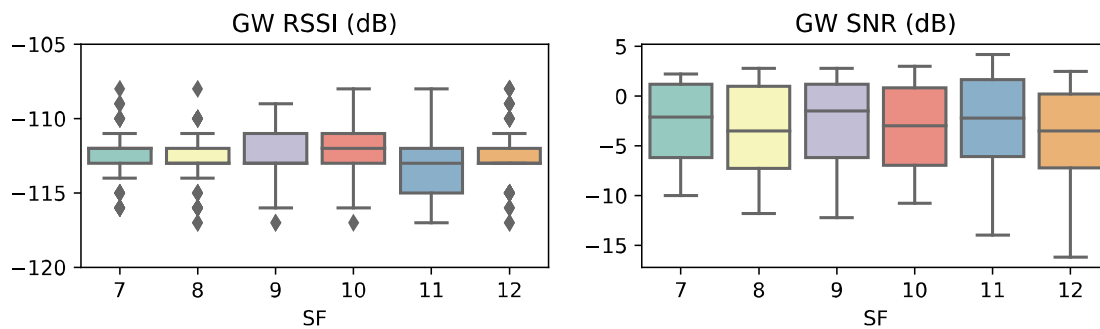


Figure 9. RSSI and SNR measurements at gateway for location 3

The results for the furthest location 3 are shown in Figure 10. For location 4 the distance was increased from 200m to 300m. The measurements for RSSI and SNR are similar to results in setup for location 3. At this location 2 packets were lost for SF of 8, while no packets were lost for all other SF.

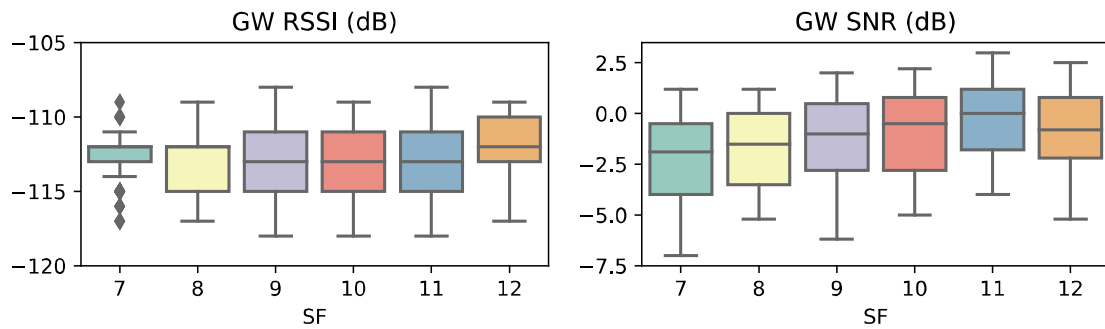


Figure 10. RSSI and SNR measurements at gateway for location 4

To sum up, the signal strength and signal to noise ratio depends on both distance between transmitter and receiver and presence of blocking objects, i.e. if we have LOS or NLOS condition. In NLOS condition the signal attenuation heavily depends of type of blocking object. Therefore, a general statement when a data transmission fails in case of NLOS can't be made. In our case, the presence of a building causing the NLOS condition as difference of scenarios location 2 and location 3 slightly lowers RSSI and SNR, but data transmission is still possible. The average RSSI over all measurements decreased by 4.2dB and the SNR by 6.49dB. This rate depends on type of object and has to be analysed for new setups. Between location 3 and 4, the distance was increased by 50%. The angle between the SN and the GW was changed, causing different objects as obstacles. The average RSSI over all measurements further declined by only 0.1dB. The average SNR even increased by 1.92dB. I.e., the increased distance does not have a significant effect. The measurements for location 3 and a SF of 12 results in a packet loss rate of 7%, while no packets were lost for smaller SF. A similar behaviour was also seen on location 4 and SF of 8. Particular spatial conditions can cause poor reception for certain SF. Then the usage of a lower SF can increase the receiving quality, although a better SNR is required for decoding. In total, transmission conditions and environments have to be analysed for new node sensor node application to select appropriate LoRaWAN transmission parameters and to ensure dependable data transmission.

## 6. BATTERY RUNTIME

The requirement for reduced maintenance demand long operating intervals between battery recharge. The proposed platform needs to compete against established products with a battery runtime of several months. Therefore, it features a low power consumption as a prerequisite. Space limitations and the used cell chemistry restrict the installable battery capacity. Nickel-metal hydride batteries show significant self-discharge over time. Lead-acid cells have a low energy density (Wh/cm<sup>3</sup>) compared to lithium-ion batteries [37]. The used lithium-ion battery combines a low self-discharge with a high energy density enabling small sensors with a long operating intervals. To optimize battery runtime a detailed power analysis of the sensor node components is performed.

### 6.1. Power Interval Analysis

The current consumption of the proposed sensor node depends on the operation state. The power consumption significantly changes between the states sensor readout, data transmission and sleep. The current consumption in all operation states was measured using a Keysight B2901A precision source measurement unit (SMU). For the measurements during the active states the supply voltage was set to 3.7V according to the nominal voltage of the used battery cell. The SF

of the SN was set to 11. The downlink messages were acknowledged by the gateway. The sampling frequency of the SMU was set to 10ms. The sensor node needs to perform an over-the-air activation (OTAA) when powering on for the first time to exchange the temporary session keys for encryption. This time-consuming procedure only needs to be repeated if the session keys are out of synchronization (e.g. the NS or AS dropped the session key). The required energy or respectively charge for the transmission of payload depends on TX power, selected SF and message type. In this example the worst case scenario with the largest possible SF, the highest allowed TX power and a confirmed uplink with acknowledge was used. The acquisition time and power consumption highly depends on the number and types of sensors that are connected. For this measurements a DHT21 temperature sensor and a BMP280 ambient pressure sensor were read out by the SN. The current consumption between the measurements is resulting from the real-time clock (RTC) of the MCU and leakage current of the circuit. The current consumption of the sensor in sleep mode is drastically reduced compared to the active states. Changes in the supply voltage show a non-negligible impact on the current consumption in sleep mode. Analysed states and related current consumptions are listed in Table 3.

Table 3. Current consumption profile

	Duration (s)	Charge (mAs)	Avg. current (mA)
<b>OTAA Join</b>	9.39	188.3	20.12
<b>Transmit</b>	2.54	67.9	26.73
<b>Acquisition</b>	0.69	10.63	15.41
<b>Sleep</b>	-	-	0.1524

## 6.2. Battery Runtime Estimation

The estimated battery runtime was estimated using the measurements from the power cycle analysis. The total charge for one cycle is calculated by Equation 2.

$$Q_{cycle} = \frac{1}{n_{rj}} Q_{join} + Q_{Acq} + Q_{TX} + I_{sleep} \cdot t_{sleep} \quad (2)$$

where,

$Q_{cycle}$  = Charge required to perform one measurement cycle

$n_{rj}$  = Average number of cycles until a re-join is required

$Q_{join}$  = Charge required for joining the network

$Q_{Acq}$  = Charge required for data acquisition

$Q_{TX}$  = Charge required for data transmission

$I_{sleep}$  = Sleep current

$t_{sleep}$  = Time between two measurement cycles

The battery runtime estimation was calculated for multiple measurement cycle times. It was assumed that a re-join is required each 20 cycles. Table 4 shows the estimated battery runtimes for various cycle times.

Table 4. Battery lifetime estimation (in days) for various cycle times

$t_{sleep}$ (m)	$Q_{cycle}$ (mAs)	$t_{battery}$ (d)
5	133,7	243
10	179,4	362
30	362,3	538

A battery runtime of almost one year was estimated when using a cycle time of 10 minutes between the measurements. This setting strikes good balance between a long battery runtime and a high sampling rate. The real battery runtime as measured is based on this cycle time.

### 6.3. Experimental Battery Runtime

The battery runtime of a SN from the first revision was measured in a long-term experiment. The SN was mounted in a greenhouse. The SN was equipped with a DHT22 temperature and relative humidity sensor and a BMP280 ambient pressure sensor, as used for the estimation. The battery voltage curve is shown in Figure 11.

The sensor was installed on 15<sup>th</sup> of January 2020 and has sent data with a cycle time of 10 minutes until 8<sup>th</sup> of September 2020, which is 237 days. The battery had an open clamp voltage (OCV) of 3.622V at the end of the experiment. The full charge of the battery could not be used due to a non-optimal power supply circuit of the used prototype. The second revision of the SN has an optimized power supply circuit supporting operation down to 3.2V OCV.

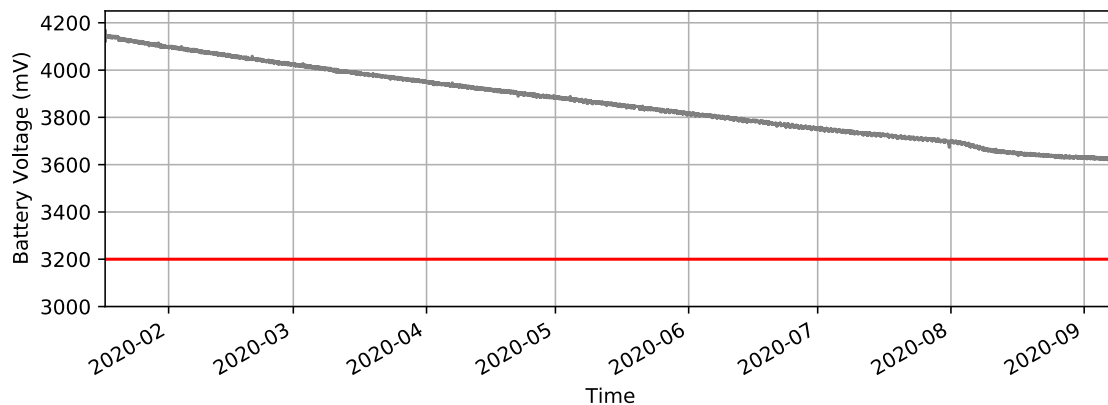


Figure 11. Battery runtime experiment for almost 8 months

## 7. SENSOR EVALUATION

For the productive use of the proposed SN it is essential that the achieved accuracy of the measurements is comparable to established products. A robust measurement of temperature and relative humidity is crucial for many UA applications. Furthermore, those measurements are well evaluable by comparison to a reference. Multiple supported sensors as listed in Table 1 were compared in terms of accuracy. The used SN was attached with two DHT22, a SHT21 and a SHT31 sensors. One of the DHT22 sensors was wrapped with a PTFE membrane as a vapour barrier to suppress condensed humidity inside the sensor. The SHT21 sensor was not equipped with a membrane and the SHT31 sensor had a factory mounted PTFE membrane. The SN was mounted outdoor next to a Pessl iMetos 3.3 weather station that was used as reference. The data was gathered over a period of 30 days. Data from the SN and the Pessl weather station was



individually transmitted with a cycle time of 10 minutes each. Both data sources are not synchronized causing a delay between both data sources.

The data was averaged over 30 minutes to compensate for time offset. The root-mean-square error (RMSE) was calculated based on the difference between the sensor readings and the reference. A linear regression was applied on the readings of each sensor and the reference. The correlation coefficient is a measure for strength of the linear correlation. The results for the temperature readings are shown in Table 5. The accuracy of the temperature sensors is quite good. Especially the cheap DHT22 sensors perform very well. The most expensive SHT31 has a small offset, but less outlier.

Table 5. Temperature measurements accuracy evaluation

Sensor	RMSE (°C)	Linearity	Offset (°C)	Corr. coeff.
DHT22	0.548	0.941	0.233	0.976
DHT22 PTFE	0.523	0.948	0.132	0.979
SHT21	0.457	0.974	0.308	0.988
SHT31 PTFE	1.134	0.962	1.119	0.978

The results for the humidity readings are represented in Table 6. The cheap DHT22 sensor with manually mounted PTFE membrane performs best. The most expensive SHT31 sensor has a poor performance.

Table 6. Humidity measurements accuracy evaluation

Sensor	RMSE (% r.H.)	Linearity	Offset (% r.H.)	Corr. coeff.
DHT22	3.612	1.382	-37.2	0.96
DHT22 PTFE	3.572	1.099	-7.67	0.933
SHT21	5.256	0.831	13.0	0.913
SHT31 PTFE	7.746	0.875	17.6	0.917

The majority of measurements is above 90% r.H. causing the relative high offset values. The linear regression would produce better results when being applied to more diversified data set. Furthermore, the data series of the sensors show a systematic error for conditions with strong solar radiation. The housing gets heated, resulting in a drop of relative humidity compared to the ambient humidity. A detailed evaluation of the humidity sensors is therefore only partly possible with the limited available data.

## 8. CONCLUSIONS

A sensor node has been developed that can be used in agriculture applications. Objectives were long range wireless communication, low-power design and modular structure to be able to easily support and to integrate different sensor devices. In this context, both, hardware and software have been optimized. The range of the developed sensor node is sufficient for urban farming applications. The distance of 300m could be bridged even with multiple buildings in between. The resulting signal quality has enough reserves for even larger distances. The results of the LOS data transmission test with a distance of 200m between sensor node and gateway show more than 20dB SNR margin, providing excellent performance application on open fields. For wireless communication a LoRaWAN modem with optimized parameter setup has been used.

The low-power feature of the sensor node has been implemented successfully, e.g. by supporting sleep modes of the processor. It was successfully verified that a battery runtime of about one year

is possible. The used battery still had some charge left after nine month of continuous operation with cycle time of ten minutes. For the first tests a non-optimal design of the power-supply circuit of the first hardware revision did not allow an operation below 3.6V battery voltage. This issue was fixed in a second hardware generation, now running down to 3.2V battery voltage. Based on the data of the first battery runtime evaluation, the revised hardware is able to operate one year on a single battery charge.

The evaluation of the supported temperature and humidity sensors show excellent results for the temperature measurements. All sensors except the SHT31 sensor showed a RMSE of around 0.5°C compared to the professional Pessl iMetos weather station. The evaluation of quality of the humidity measurements was partially possible only, because the humidity was almost above 90% r.H. during the whole test period. It was shown that the cheap DHT22 sensor with a manually attached PTFE membrane performs very good. In contrast, the expensive SHT31 showed a poor performance during the test period. The high accuracy and the reasonable costs of the DHT22 sensor supports the large-scale deployment of the proposed SN in UA applications.

The proposed sensor node is suitable for field soil measurements, aquaponics monitoring and urban farming applications. The long battery runtime and the continuous data transmission provide benefits compared to the usage of traditional offline or cellular data loggers. The extended range is sufficient for covering large areas under LOS conditions. A single gateway is able to cover a large field, eliminating e.g. the need to use UAV solutions to locally read sensor data.

### 8.1. Further Research

The collected data series of humidity measurements did not cover the full value range. The accuracy of the used sensor could be further evaluated using a more comprehensive data set. The construction of the sensor housing was not optimal. Solar radiation heated the housing causing a drop in relative humidity compared to ambient humidity. So far, only the accuracy of temperature and humidity measurements was evaluated. More sensors for measuring e.g. ambient pressure, light irradiation, and pH value need to be assessed in future research. The suitability of the proposed sensor node for application on large fields, e.g. soil measurements, could be further proved by experiments in large scale real-world scenarios. Further research could evaluate the usage of 5G technology as a replacement for the used LoRaWAN technology with the proposed sensor node architecture. This cellular technology would eliminate the need for a stationary gateway. The required power consumption needs to compete with the LoRaWAN solution to allow a comparable battery lifetime.

### REFERENCES

- [1] S. M. Vicente-Serrano, F. Domínguez-Castro, C. Murphy, J. Hannaford, F. Reig, D. Peña-Angulo, Y. Trambly, R. M. Trigo, N. M. Donald, M. Y. Luna, M. M. Carthy, G. V. D. Schrier, M. Turco, D. Camuffo, I. Noguera, R. García-Herrera, F. Becherini, A. D. Valle, M. Tomas-Burguera, and A. E. Kenawy, "Long-term variability and trends in meteorological droughts in Western Europe (1851–2018)," *International Journal of Climatology*, vol. 41, no. S1, 2020.
- [2] R. Christensen, "SPIN-Farming: advancing urban agriculture from pipe dream to populist movement," *Sustainability: Science, Practice and Policy*, vol. 3, no. 2, pp. 57–60, 2007.
- [3] O. Elijah, T. A. Rahman, I. Orikumhi, C. Y. Leow, and M. N. Hindia, "An Overview of Internet of Things (IoT) and Data Analytics in Agriculture: Benefits and Challenges," *IEEE Internet of Things Journal*, vol. 5, no. 5, pp. 3758–3773, 2018.
- [4] A. Goldstein, L. Fink, A. Meitin, S. Bohadana, O. Lutenberg, and G. Ravid, "Applying machine learning on sensor data for irrigation recommendations: revealing the agronomist's tacit knowledge," *Precision Agriculture*, vol. 19, no. 3, pp. 421–444, 2017.

- [5] T. Machl and T. Kolbe, "Analyse landwirtschaftlicher Transportbeziehungen", Wege mit Zukunft, 2017.
- [6] K. Bradley, "Micro-farming on Rented Land: Curtis Stone Interview", Kewlona, 2017.
- [7] A. Farhad, D.-H. Kim, and J.-Y. Pyun, "Scalability of LoRaWAN in an Urban Environment: A Simulation Study," 2019 Eleventh International Conference on Ubiquitous and Future Networks (ICUFN), 2019.
- [8] Onset, "U30 USB Weather Station," HOBO U30-NRC datasheet, 2021
- [9] Gemini, "Tinytag Plus 2 Dual Channel Temperature/Relative Humidity", TGP-4500 datasheet, Oct. 2014
- [10] R. Shaw, R. Lark, A. Williams, D. Chadwick, and D. Jones, "Characterising the within-field scale spatial variation of nitrogen in a grassland soil to inform the efficient design of in-situ nitrogen sensor networks for precision agriculture," Agriculture, Ecosystems & Environment, vol. 230, pp. 294–306, 2016.
- [11] S. Chatterjee, N. Dey, and S. Sen, "Soil moisture quantity prediction using optimized neural supported model for sustainable agricultural applications," Sustainable Computing: Informatics and Systems, 2018.
- [12] J. P. Becona, A. S. Pereira, C. Vazquez, and A. Arnaud, "A battery powered RTU: GPRS vs 3G comparison: IEEE Urucon 2017 paper 101," 2017 Ieee Urucon, 2017.
- [13] R. Yordanov, R. Miletiev, P. Kapanakov and E. Lontchev, "Design of a portable system for sensor data acquisition and transmission," 2017 XXVI International Scientific Conference Electronics (ET), Sozopolpp. 1-3, 2017.
- [14] A. D. Zayas and P. Merino, "The 3GPP NB-IoT system architecture for the Internet of Things," 2017 IEEE International Conference on Communications Workshops (ICC Workshops), 2017.
- [15] J. Zhang, P. Liu, W. Xue, and Z. Rui, "Farmland Intelligent Information Collection System Based on NB-IoT," Cloud Computing and Security Lecture Notes in Computer Science, pp. 331–343, 2018.
- [16] "Telekom LTE NB-IoT Coverage Map for Germany" [Online]. Available: <https://t-map.telekom.de/tmap2/nbiot>. [accessed: 23-Jan-2021].
- [17] "SigFox Coverage Map" [Online]. Available: <https://www.sigfox.com/en/coverage>. [accessed: 23-Jan-2021].
- [18] X. Zhang, A. Andreyev, C. Zumpf, M. C. Negri, S. Guha and M. Ghosh, "Thoreau: A subterranean wireless sensing network for agriculture and the environment," 2017 IEEE Conference on Computer Communications Workshops (INFOCOM WKSHPs), Atlanta, GA, pp. 78-84 , 2017.
- [19] L. Joris, F. Dupont, P. Laurent, P. Bellier, S. Stoukatch, and J.-M. Redoute, "An Autonomous Sigfox Wireless Sensor Node for Environmental Monitoring," IEEE Sensors Letters, vol. 3, no. 7, pp. 01–04, 2019.
- [20] J. Chen, Z. Dai, and Z. Chen, "Development of Radio-Frequency Sensor Wake-Up with Unmanned Aerial Vehicles as an Aerial Gateway," Sensors, vol. 19, no. 5, p. 1047, Jan. 2019.
- [21] A. Rajakaruna, A. Manzoor, P. Porambage, M. Liyanage, M. Ylianttila, and A. V. Gurtov, "Lightweight Dew Computing Paradigm to Manage Heterogeneous Wireless Sensor Networks with UAVs", ArXiv, 2018.
- [22] A. Noriega and R. Anderson, "Linear-Optimization-Based Path Planning Algorithm for an Agricultural UAV," AIAA Infotech @ Aerospace, 2016.
- [23] L. H. Nam, L. Huang, X. J. Li and J. F. Xu, "An approach for coverage path planning for UAVs," 2016 IEEE 14th International Workshop on Advanced Motion Control (AMC), Auckland, pp. 411-416, 2016.
- [24] M. Idbella, M. Iadaresta, G. Gagliarde, A. Mennella, S. Mazzoleni, and G. Bonanomi, "AgriLogger: A New Wireless Sensor for Monitoring Agrometeorological Data in Areas Lacking Communication Networks," Sensors, vol. 20, no. 6, p. 1589, 2020.
- [25] N. H. N. Ibrahim, A. R. Ibrahim, I. Mat, A. N. Harun, and G. Witjaksono, "LoRaWAN in Climate Monitoring in Advance Precision Agriculture System," 2018 International Conference on Intelligent and Advanced System (ICIAS), 2018.
- [26] D. Davcev, K. Mitreski, S. Trajkovic, V. Nikolovski, and N. Koteli, "IoT agriculture system based on LoRaWAN," 2018 14th IEEE International Workshop on Factory Communication Systems (WFCS), 2018.
- [27] Semtech, "AN1200.22", LoRa Modulation Basics, 2015.
- [28] LoRa Alliance, "LoRaWAN 1.1 Specification", 2017.
- [29] Node-RED, "About", [Online] Available: <https://nodered.org/about/>. [accessed: 29-Jan-2021].

- [30] D. Arnst, V. Plenk, A. Woeltche., "Comparative Evaluation of Database Performance in an Internet of Things Context", 2018.
- [31] Grafana Labs, "Grafana Features", [Online] Available: <https://grafana.com/grafana/>. [accessed: 29-Jan-2021].
- [32] P. Bolte and U. Witkowski, "Energy self-sufficient sensor node for long range wireless networks," IOP Conference Series: Earth and Environmental Science, vol. 431, 2020.
- [33] Semtech, "AN1200.13", SX1272/3/6/7/8 LoRa Modem Designer's Guide, 2013.
- [34] Semtech, "RP002-1.0.0", LoRaWAN Regional Parameters, 2019.
- [35] Wifx, "Compact and Robust Professional Grade LoRaWAN Gateway", LORIX One, 2020.
- [36] T. Elshabrawy and J. Robert, "Analysis of BER and Coverage Performance of LoRa Modulation under Same Spreading Factor Interference", 2018 IEEE 29th Annual International Symposium on Personal, Indoor and Mobile Radio Communications (PIMRC), 2018.
- [37] S. Anuphappharadorn, S. Sukchai, C. Sirisamphanwong, and N. Ketjoy, "Comparison the Economic Analysis of the Battery between Lithium-ion and Lead-acid in PV Stand-alone Application," Energy Procedia, vol. 56, pp. 352–358, 2014.

## AUTHORS

**Philipp Bolte** is research assistant at the Department of Electronics and Circuit Technology of the South Westphalia University of Applied Sciences since 2016. He received his master's degree in systems engineering in 2017. Currently, he is working on his PhD research with focus on industrial IoT sensor nodes.



**Dr. Ulf Witkowski** heads the Electronics and Circuit Technology research group at the South Westphalia University of Applied Sciences in Soest, Germany. He has been an active researcher for about 20 years in the area of wireless networking, sensor networks, cognitive systems, and mini-robotics. He has established his research group at the South Westphalia University as a professor in 2009. His research areas include wireless communication involving mobile ad-hoc networking, radio-based node localization, sensor networks, and embedded systems. He received the diploma degree in electrical engineering in 1995 from the Technical University of Hamburg-Harburg, Germany and in 2003 the Dr.-Ing. degree from the University of Paderborn. U. Witkowski has published more than 80 scientific articles.



Chemical engineer **Rolf Morgenstern** (51), started researching sustainable food production, focussing on Urban Agriculture and Aquaponics, at the department of agriculture of SWUAS in 2015.

